INHIBITORY EFFECT OF AZA-MACROCYCLIC LIGANDS ON POLYPHENOL OXIDASE IN MODEL AND FOOD SYSTEMS.

Sara Muñoz-Pina[1], José V. Ros-Lis[2]*, Estefanía Delgado-Pinar[3]*, Álvaro Martínez-Camarena,[3] Begoña Verdejo[3], Enrique García-España[3], Ángel Argüelles[1], Ana Andrés[1]

[1] Instituto Universitario de Ingeniería de Alimentos para el Desarrollo (IUIAD-UPV). Universitat Politècnica de València Camino de Vera s/n, 46022, Valencia, Spain.

[2] REDOLí, Departamento de Química Inorgánica, Universitat de València, 46100, Burjassot, Valencia Spain.

[3] Instituto de Ciencia Molecular, Universidat de València. C/Catedrático José Beltrán 2, Paterna (Valencia), Spain.

*Corresponding author. Email: J.Vicente.Ros@uv.es; Estefania.Delgado@uv.es

ABSTRACT

Enzymatic browning is one of the main problems faced by the food industry due to the enzyme polyphenol oxidase (PPO) action provoking undesirable colour change in the presence of oxygen. Here, we report the evaluation of ten different azamacrocyclic compounds with diverse morphologies as potential inhibitors against the activity of PPO, both in model and real systems. An initial screening of ten ligands show that all aza-macrocyclic compounds inhibit to some extent the enzymatic browning, but the molecular structure plays a crucial role on the power of inhibition. Kinetic studies of the most active ligand (L2) reveal a S-parabolic I-parabolic non-competitive inhibition mechanism and a remarkable inhibition at micromolar concentration (IC_{50} = 10 μM). Furthermore, L2 action has been proved on apple juice significantly reducing the enzymatic browning.

Key words: PPO, inhibition, macrocyclic polyamines, enzymatic activity

1. Introduction

There is currently a growing tendency to consume fresh, cut, ready-to-eat fruits and vegetables or minimally processed fresh juices as there is a great concern for maintaining a healthy diet and preserve their sensory and nutritional properties. Therefore, maintaining the stability of the product and ensuring the natural colour is one of the main objectives of the food industry [1,2].

The main cause of colour modification of fruits and vegetables can be associated to the activity of enzyme polyphenol oxidase (PPO, EC 1.14.18.1 or EC 1.10.3.1). The PPO catalyse the *o*-hydroxylation of monophenols into *ortho*-phenols and its posterior oxidation to *o*-quinones followed by a non-enzymatic polymerization of reactive quinones leading to the enzymatic browning of foods[3]. This reaction starts when the PPO enzyme and the atmospheric oxygen meet, usually during cell disruptions of the raw food in their harvesting, handling and post-harvest processing. The colour change, yet it is a desirable process in some foods[4], is inversely correlated with the acceptability of fruit and vegetable products by the consumer[5] which causes a considerable increase in food waste economic losses[6,7].

Since the factors that most influence enzymatic browning are the concentration of both the active enzyme and the phenolic compounds (plus the pH, the temperature and the presence of oxygen)[8] the processing of foods with high concentrations of PPO and polyphenols leads to a high risk of enzymatic browning in this type of food. A clear example would be the case of apple juices, which contain considerable amounts of polyphenols and polyphenol oxidases linked to suspended particles[9].

Food waste is a major humanitarian and environmental problem (Food and Agriculture Organization of the United Nations, 2011)[10] so it is not unexpected that food processing industry has been using different methods to prevent the enzymatic browning based on both physical and chemical treatments. Traditionally, one of the methods most used by the industry has been the thermal treatment. But heat induces changes in taste, colour, smell and nutritional properties due to the decomposition of volatile and thermosensitive compounds, such as aromas, vitamins, carotenoids and anthocyanins[11,12]. Regarding chemical treatments, the use of acidifying agents, chelators or sulphites have also been used as preventive for browning, but the fact that they can interfere with the taste or even cause allergies in the population (sulphites) has restricted their use in foods and beverages [13,14]. These drawbacks encourage researchers to still look for a novel strategies of PPO inhibitors, as could be the use of the nanomaterial technology[15,16].

From another point of view, supramolecular chemistry is a research subject of great interest at present. It studies the non-covalent interactions between molecules, usually named host and guest. The host molecules, in general, are large molecules capable of enclosing smaller molecules and they can be natural, semi-synthetic or completely synthetic molecules. On the other hand, the smaller guest molecules can be cationic, anionic or neutral like amino acids, organic anions and some metals[17].

Within the receptors designed for supramolecular studies, macrocyclic polyamines are especially relevant[18]. Polyamines offer a high potential as PPO inhibitors since these compounds can interact with metal cations with biological relevance such as Cu^{+2} [19–21] and have also the ability to interact with amino acids through hydrogen bonds or electrostatic interactions. In addition, these ligands can be functionalized with different

chemical groups like aromatic groups or alkyl groups that can change their response over the PPO.

So far there are no studies aimed at studying the interactions between this type of compounds and polyphenol oxidase as a strategy for their inhibition in food systems. We can hypothesize that azamacrocycles can interact with the copper atoms in the active centre of the external part of the enzyme modifying its activity. Therefore, this work aims at analyse the behaviour of different azamacrocyclic compounds in the inhibition or modulation of the polyphenol oxidase enzyme activity in model and real systems, as starting point to develop an alternative strategy for the industrial processing of fruits and vegetables.

2. **Materials and methods**

2.1. Chemicals

Commercial mushroom tyrosinase enzyme (2687 U/mg), dopamine hydrochloride ($(HO)_2C_6H_3CH_2NH_2 \cdot HCL$) and HEPES ($C_8H_{18}N_2O_4S$) were purchased all from Sigma-Aldrich (Sigma-Aldrich, USA). For the buffers, sodium bisphosphate (NaH_2PO_4) and disodium phosphate (Na_2HPO_4) were acquired from Scharlau (Sharlab S.L., Spain) and anhydrous sodium acetate ($NaCH_3COO$) from Panreac AppliChem (Panreac AppliChem, Barcelona, Spain).

The ligand S1 (cyclam) was purchased from Sigma-Aldrich (Sigma-Aldrich, USA). The others tested ligands were synthesised according to known procedures and the characterisation agrees with published data: S2[22], S3[23], S4[24], M1[25], M2[26], M3[27], L1[28], L2[29] and L3[30]. The different chemical structures are summarized in Scheme 1.

The juices used in the tests were obtained in the laboratory by directly liquefying apples (Golden Delicious variety, Val Venosta) obtained in a local store.

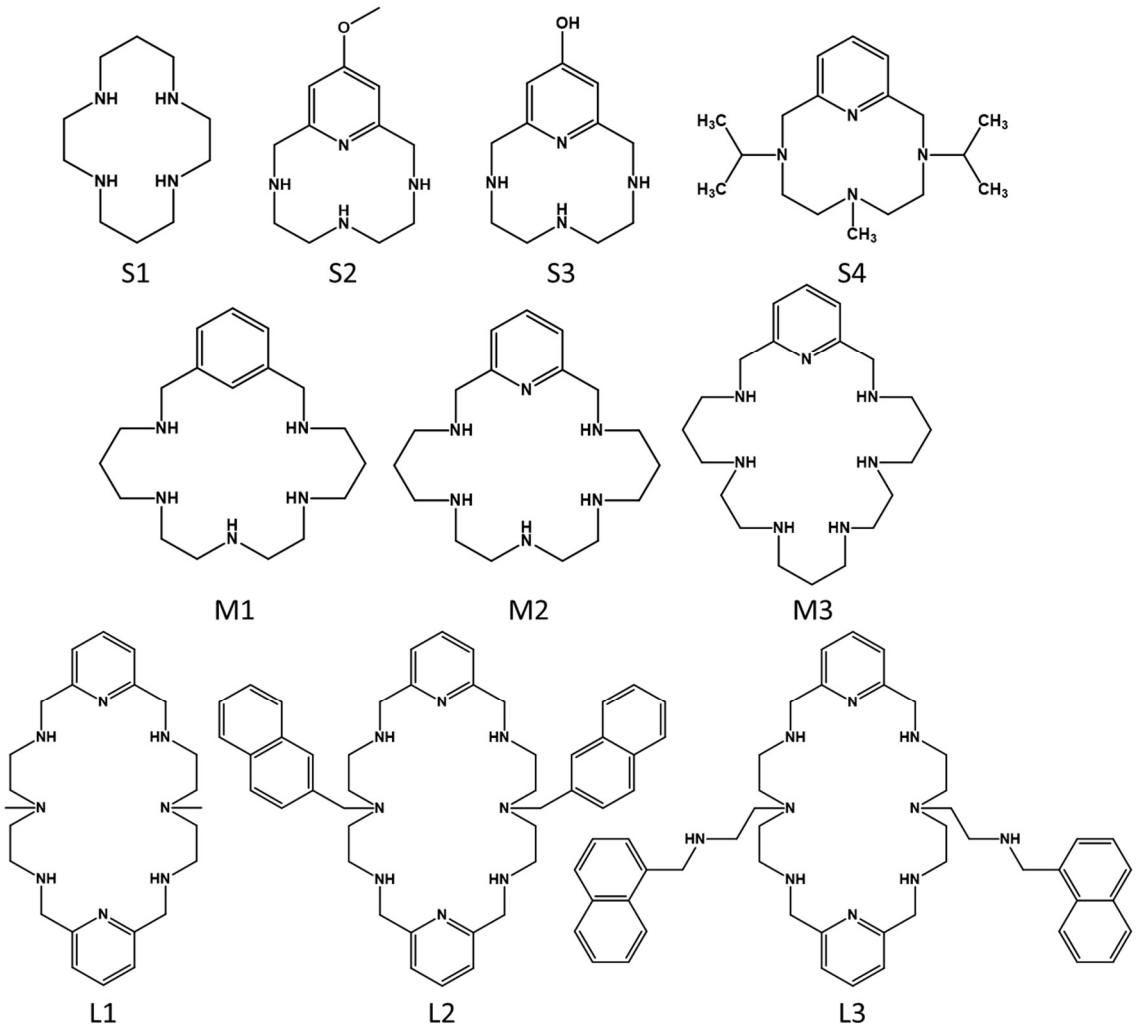

Scheme 1: Molecular structure of the ten studied azamacrocyclic ligand

2.2. Screening of the best inhibitors over tyrosinase from mushroom

Polyphenol oxidase activity in the presence of the ligands was determined following the protocol published by Muñoz-Pina et al.(2020)[16] and with some modifications from Siddiq and Dola (2017)[31]. Tyrosinase from mushroom (93.75 U) was put in contact with dopamine (2.5 mM) in presence of the ligand (0.67 mM) in a phosphate buffer 10 mM at pH 5.5. A control without inhibitor was used. The oxidation of the dopamine by the PPO produces an orange colour that is followed spectrophotometrically at 420 nm measuring the absorbance each 10 s during 10 min. From the absorption-time curves,

the slope of the linear stretch is obtained, related to the initial speed of the reaction. The different slopes were used to compare the inhibitory effect of the ligands against the control (see equation 1). The reaction was followed by a Beckman Coulter DU-730 Life Science UV/Vis spectrophotometer in triplicate at 24 °C. PPO inhibition was calculated according to Eq. (1), where V_{o0} is the control initial rate and V_{oi} is the initial rate obtained for the different samples.

$$PPO\ inhibition\ (\%) = 100 - \left(\frac{V_{0i}}{V_{00}} * 100\right) \qquad (1)$$

2.3. Enzyme-ligand interaction

To evaluate the influence of the contact time between the enzyme and the ligands, the enzyme was put in contact with the ligand at time 0 min and at 60 min. The azamacrocyclic compounds selected for the assay were M1, M2, M3, L2 and L3 (all at 0.67 mM). The reaction mixture was the same as in 2.2 and in both times a control without inhibitor was prepared.

The absorbance was then measured at 420 nm every 10 s for 10 min in a Beckman Coulter DU-730 Life Science UV/Vis spectrophotometer and the effect of the contact time on the initial rate was compared. PPO inhibition was calculated according to Eq. (1), where V_o0 is the control initial rate and V_oi is the initial rate obtained for the different samples.

Also, the oxygen potential was measured over the reaction time to determine the oxygen consumption. Oxyview 1 measuring system of Hansatech Instruments was used, which contains a S1 Clark-type polarographic oxygen electrode disc mounted within a DW1/AD electrode chamber and connected to the Oxyview electrode control unit. The oxygen consumption vs time curve was plotted and the positive slope of the initial part, considered as the initial rate of oxygen consumption, was calculated and compared with

the results of the selection test. PPO inhibition was calculated then according to Eq. (1), where V_o0 is the control positive initial rate of oxygen consumption and V_oi is the initial rate of oxygen consumption obtained for the different samples.

2.4. Enzyme kinetics in model systems

The five compounds with more inhibitory capacity were chosen to make a deeper study of enzymatic activity. For the determination of the kinetic parameters, the reaction was carried out at pH 5.5 under phosphate buffer 10 mM at ten different concentrations of the substrate dopamine (from 0.033 mM to 1.66 mM). The final concentration of enzyme in the assay was 93.75 U and the inhibitor concentration varied depending of its response. A control without inhibitor was also carried out. The absorbance at 420 nm was measured every 10 s for 10 min in a Spectrophotometer Beckman Coulter DU-730 Life Science UV / Vis Spectrophotometer. The production of dopamine was determined using a molar extinction coefficient for dopachrome of $\varepsilon = 3700\ M^{-1}\ cm^{-1}$ [32].

Since the enzymatic reaction of polyphenol oxidase follows a kinetics of Michaelis Menten[33], K_M and v_{max} constants were calculated using the Lineweaver-Burk representation as a linearization method and compared to the representation of Langmuir[34]. The type of inhibition was also determined. Besides, GraphPad Prism 5.00.288 program was used to carry out various statistical analyses such as the analysis of variance (ANOVA) of one factor and two factors, depending on the case.

2.5. Fluorescence quenching analysis

The fluorescence assay was performed with a PTI fluorescence instrument. Same inhibitor/enzyme mixture as in section 2.2. was used in this study at the three ligand concentrations. Tyrosinase was excited at 274 nm and the emission spectrum over the

155 range of 280 nm to 400 nm was recorded through a 3 nm slit. The emission spectrum of
156 the tyrosinase solution was also directly measured.

157 2.6. Inhibitory effect over apple juice

158 Apple juice from cv. Golden Delicious obtained in the laboratory was selected to verify
159 their inhibitory effects of the compounds on real samples. For each compound, a 2 mL
160 aliquot of juice was put in contact with 2 mg and 4 mg of compound and another 2 mL
161 of apple juice was used as a control sample. All samples were kept under agitation (400
162 rpm) for 60 minutes and photographs were taken at 0, 1 and 2 minutes and then at 5-
163 minute intervals, in order to monitor and visualize the enzymatic browning.
164 Furthermore, CIE L*a*b* (CIELAB) coordinates were measured in the images and colour
165 differences were calculated using Adobe® Photoshop®.

166 2.7. Data analysis

167 Data are reported as mean ± standard deviation. Origin was used to perform the analysis
168 of variance (One-Way ANOVA) and the LSD procedure (least significant difference).
169 Partial least squares regression studies (PLS) were carried out with the R 3.6.0 software
170 using the Kernel algorithm. Scale and center were used as parameters to build the
171 model. Leave one out (LOO) cross-validation was used to evaluate the adequacy of the
172 experimental data and to select the quantity of latent variables.

173 **3. Results and discussion**

174 3.1. Selection of the best inhibitors

175 A macrocyclic ligand can interact directly with enzymes via supramolecular interactions,
176 but at the same time, it is able to bind a metal atom within its central cavity. Besides,
177 this cavity can be branched or functionalized with other chemical groups to stimulate
178 the interactions with further spices as enzymes[24]. The size and spatial arrangement of

179 the coordinating groups are of great importance since it significantly influences the
180 properties of the complexes and this affects their selectivity[35]. First on this study diverse
181 compounds with different chemical structures were chosen in order to evaluate the
182 effect of their presence in the oxidation reaction of dopamine by polyphenol oxidase
183 (see scheme 1). The selected compounds have in common a macrocyclic unit. The size
184 of the cavity varies depending of the number of atoms in the ring. Therefore, for clarity
185 in the discussion, the ligands were divided according to the number of nitrogen groups
186 in the macrocycle in small (S1, S2, S3, and S4), medium (M1, M2, and M3) and large (L1,
187 L2, and L3).
188 An initial screening of the inhibitory activity was accomplished measuring the
189 absorbance at 420 nm in presence of the ligand at pH 5.5 with dopamine as a substrate
190 (Figure 1). In general terms, all the ligands reduce the initial reaction rate, which can be
191 translated as a partial inhibition of the enzymatic activity. The degree of inhibition varies
192 strongly among the ligands with a decrease in the initial PPO rate from 11.4 to 94.5 %
193 depending on the chemical structure. %. On a fist sight, it can be seen how smallest
194 cycles (S1, S2, S3, and S4) were not able to reduce the enzymatic activity of the PPO
195 more than 40%. Besides, M1, M2, and M3, bigger in structure, presented better
196 inhibition power with M3 inhibiting 70% the PPO activity. Finally, L2 induces the greatest
197 inhibition over the PPO (almost 95%) seeming that the functionalization with the two
198 naphth-2-ylmethyl plays an important role. However, not only the naphth-2-ylmethyl
199 units makes the difference as L3 present less inhibition (70%) having the same units but
200 with an amine between the macrocycle and the naphthalene.
201 If we compare these values with those reported by Wei Liu and co-workers[36] using citric
202 acid as a typical tyrosinase inhibitor we can observe that these ligands present higher

power of inhibition. In the case of citric acid, it was necessary a concentration superior to 10 mM to reach an inhibition of the 20% over tyrosinase from mushroom. They also report that the minimum of citric acid was 10 mM to strongly inhibit the PPO from bananas. Even though this behaviour depends on the substrate source (catechol vs dopamine), in our case all the ligands present 10 times superior inhibition power with only 0.67 mM. Regarding to others commonly used organic acids, such as oxalic acid, Son et al., [37] pointed out that a concentration of approximately 1 mM could inhibit the PPO in a 50% and 5 mM to reach the 80%. Similar behaviour is reported for benzoic acid[38] over mushroom PPO where in needed a concentration of 5.20 mM to reach the 50% of inhibition. In our case most of the ligands from the M and L family reporter greatest inhibitory force as they need less concentration than 1 mM to reach more than the 50%.

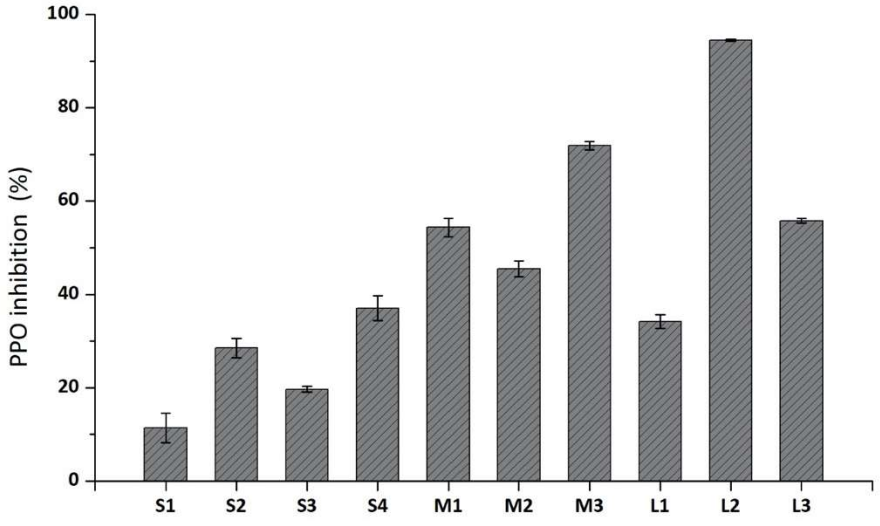

Figure 1: Polyphenol oxidase (94 U) inhibition in presence of the ten different azamacrociclic ligand (0.67 mM) using dopamine as substrate (2.5 mM).

In order to gain insight about the influence of the chemical structure in the PPO activity, the ligands were parametrised (see table 1) and the degree of inhibition modelized with the Partial Least Squares Regression (PLS) technique. The PLS is a multivariate projection method that models the relation between an array of dependent variables (Y) and another array of independent variables (X) to find the components that allow the highest correlation with Y. In our case the independent variables were the parametrised data contained in the Table 1 and the dependent variable was the degree of inhibition shown in the Figure 1. All the data/ligands were included in the training set because the number of molecules was small, and we were interested in understanding the influence of the functional groups in the inhibitory activity measured during the screening.

Table 1: Parametrised values of the ligands used in the PLS and squared values of the first four principal components.

Ligand / Loading	Ntot[a]	Pyr[b]	NH[c]	Nter[d]	Ant[e]	Amac[f]	OH[g]	Met[h]	Nmac[i]	Rsize[j]	Benz[k]	Sch[l]	Lch[m]	Inhib[n]
S1	4	0	4	0	0	0	0	0	4	14	0	0	0	11,4
S2	4	1	3	0	0	0	0	1	4	12	0	0	0	28,5
S3	4	1	3	0	0	0	1	0	4	12	0	0	0	19,7
S4	4	1	0	3	0	0	0	0	4	12	0	1	2	37,1
M1	5	0	5	0	0	0	0	0	5	20	1	0	0	54,4
M2	6	1	5	0	0	0	0	0	6	20	0	0	0	45,5
M3	7	1	6	0	0	0	0	0	7	24	0	0	0	71,4
L1	8	2	4	2	0	0	0	0	8	24	0	2	0	34,2
L2	8	2	4	2	2	2	0	0	8	24	0	0	2	94,5
L3	10	2	6	2	2	0	0	0	8	24	0	0	2	55,8
PC1[+]	0,1								0,08	0,77				
PC2[+]		0,05	0,52*	0,48	0,15	0,12				0,05*			0,45	
PC3[+]	0,16*	0,09*	0,19	0,29*					0,06*			0,16*		
PC4[+]	0,43*		0,61*		0,36*					0,21		0,26	0,13*	

[a] Ntot: total number of nitrogens. [b] Pyr: number of pyridine units. [c] NH: number of NH groups [d] Nter: number of tertiary amines [e] Ant: number of anthracene units [f] Amac: number of anthracene units attached to the macrocycle. [g] OH: number of OH groups. [h] Met: number of methoxy groups. [i] Nmac: number of N in the macrocycle. [j] Rsize: number of atoms that compose the macrocycle. [k] Benz: number of benzene units. [l] Sch: number of small chains attached to the macrocycle. [m] Lch: number of big chains attached to the macrocycle. [n] Inhib: % of inhibition calculated as 100-

239 initial PPO rate. + Values lower than 0,05 have been omitted for clarity. * loadings with negative

240

241 To check the quality of the model the Leave One Out (LOO) method was used and 4
242 latent variables selected. Figure 2 contains a graph with the measured vs. the predicted
243 values of the inhibitory activity for each ligand. The measured and predicted values were
244 plotted together to evaluate the accuracy and precision of the created prediction
245 models. Ideally, the predicted values should lie along the diagonal line, indicating that
246 the predicted and actual values are the same. As can be seen in Figure 2, in general a
247 good fit is obtained and most of the points remain next to the solid line. Furthermore,
248 a linear fitting of the by using of the points in the graph with a simple linear model (y =
249 ax + b) offered values of 0.915, 3.86 and 0.915 for the slope, the intercept and R^2
250 respectively.

251

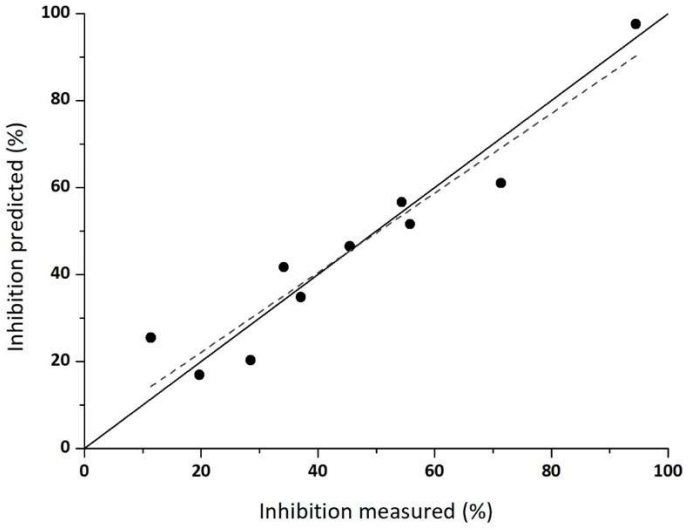

252

253 Figure 2: Experimental versus predicted values by using a PLS statistical model (dashed
254 lines) for the PPO inhibition. The solid line represents ideal behaviour.

255

The effect of the chemical structure parameters defined in the table 1 in the inhibitory activity, was analyzed from the squared loadings for the first four principal components (PCs) (Table 1). In PLS the first principal component (PC1) contains the highest explained variance and explains most of the inhibitory response, next PC2 and so on. In this case, PC1 suggest that the ring size is the main factor responsible of the inhibitory response. Also, high values are found for the total number of nitrogens (Ntot) and the number of nitrogens in the macrocyle (Nmac), suggesting that together with the ring size, the amino groups are highly relevant for the inhibitory activity. However, as the number of nitrogen atoms in the ligand is high correlated with the macrocycle size, the inhibitory effect can be assigned neither to the ring size nor to the total number of nitrogens separately.

As can be seen in the table 1, we can assign as a second main factor in the ligands activity (PC2) to the macrocycle functionalization (Nter, Ant, Amac), with preference for the big size substituents (Lch) over the little groups (Sch). Also, the presence of the pyridine moiety seems improve the response. Regarding the other two principal components, the number of NH (PC3) and methyl groups (PC4) have a positive but minor effect. Other functional groups such as the presence of benzene, the hydroxy or methoxy groups do not seem offer any advantage.

From the structure of the ligands and the PLS analysis we can conclude that the key factor of the inhibitory activity is the presence of a big macrocycle containing several amino groups and it improves with the presence of bulky hydrophobic substituents (i.e. i-Pr or anthracene) directly attached to the ring.

3.2. Ligand-PPO interaction

Since the ligands M1, M2, M3, L2, and L3 had reported the greatest power of inhibition over the PPO (at least 50%), we selected them to analyse their interaction more thoroughly.

As previously mentioned, the enzymatic browning process comprises two phases, firstly, the enzymatically catalysed oxidation takes place, followed by a non-enzymatic polymerization reaction that generates the brown colour [39]. Although the appearance of colour is generally used to follow the enzymatic browning reaction, the speed of oxygen consumption allows us to prove that the effect of azamacrocyclic compounds is directly related to the enzymatic activity (oxidation) and not associated with the non-enzymatic polymerization of the quinones.

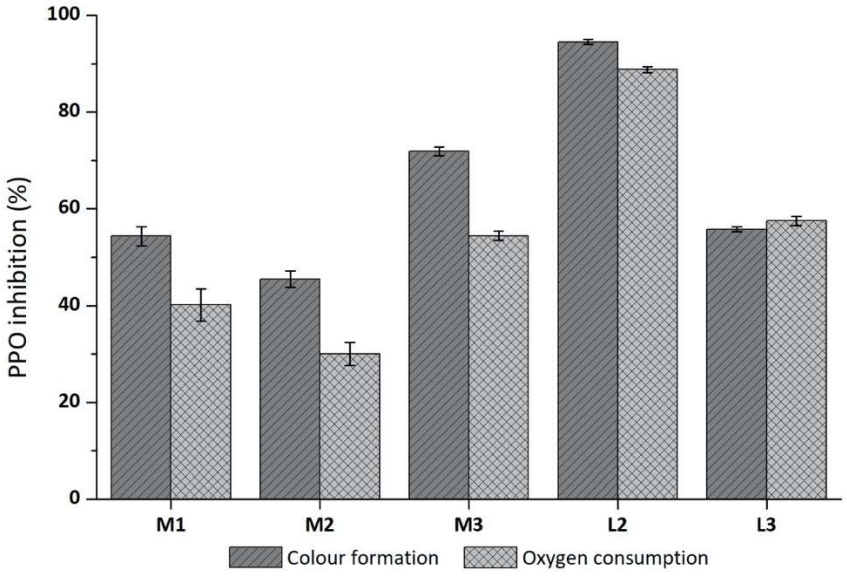

Figure 3: PPO (94 U) inhibition (%) based on colour formation (light grey) and based on oxygen consumption (dark grey) for the five selected ligands (0.67 mM).

As seen in figure 3, the initial rates of oxygen consumption and colour formation were compared for the five inhibitors selected. Despite being different methodologies, both techniques reveal an appreciable increase on the inhibition of the browning process. The behaviour observed is that, although similar, the inhibition over the colour formation is higher than the inhibition of the oxygen consumption. This suggests that their mechanisms would not only involve with the enzyme, but an interfere with the polymerization reaction. By contrast, L2 shows a slight variance (5%) between both techniques and L3 does not show any meaningful difference between the initial velocity of oxygen consumption and colour formation. These results suggest that for L2 and L3 the decrease in browning is mainly due to a decrease in the PPO activity.

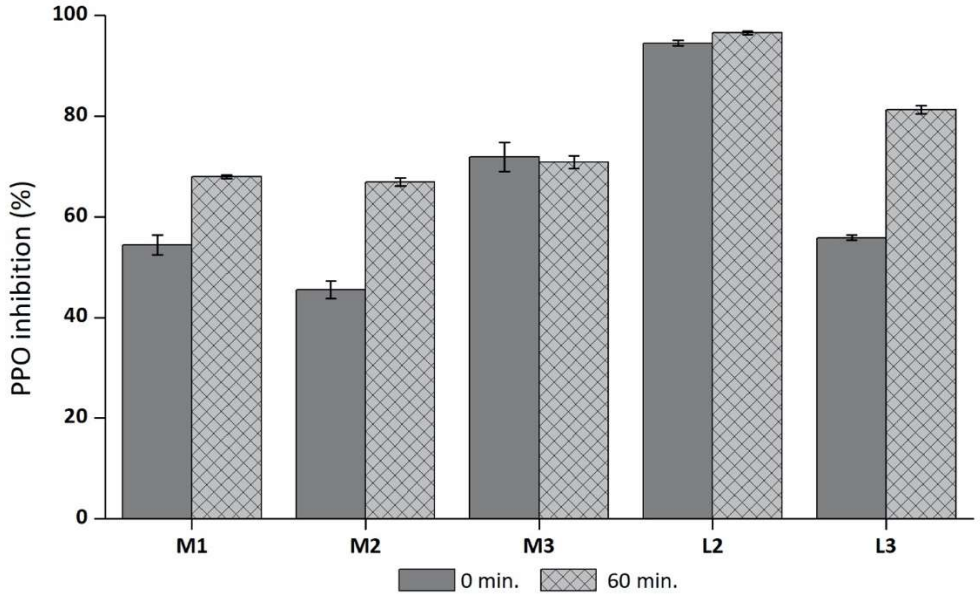

Figure 4: Effect of contact time between polyphenol oxidase (94 U) and the different ligands on their inhibitory capacity prior to substrate addition. Without previous contact time (0 min; dark grey) and with 60 minutes of previous contact time (light grey).

Furthermore, the influence of the contact time between the enzyme and the different compounds should be considered as it might affect the inhibitory capacity over the PPO. Thus, it was analysed the response of the five selected ligands varying the previous contact time between the ligand and the PPO prior to substrate addition (0 min and 60 min). With the exception of M3 (see figure 4), the speed decreases as the contact time increases being the differences significant ($p < 0.0001$). This would indicate that if the enzyme and the inhibitor are previously in contact in solution, they are able to interact to a greater extent, obtaining higher inhibition values.

3.3. Kinetic parameters determination

As tyrosinase from mushroom follows Michaelis-Menten kinetics, in order to understand and compare the nature of the enzyme-inhibitor interaction, the classical method of Lineweaver-Burk plots was used to determine the kinetic parameters and the inhibition mechanism for each inhibitor (see table 2).In the case of the Michaelis-Menten K_m constant, the value for the control was K_M = 1.05 ± 0.05 mM and 0.3321 $mMmin^{-1}$ for v_{max}.

Table 2: Kinetic parameters and type of inhibition of the enzyme Tyrosinase from mushroom (94 U) in presence of the five selected ligands at different concentrations.

Compound (mM)		K_M[a] (mM)	v_{max}[b] (mM min^{-1})	k_{cat}[c] (min^{-1})	Catalytic efficiency[d] (mM^{-1} min^{-1})	IC_{50} (mM)	K_i (mM)	Inhibition type
Control		1.05 ± 0.05*	0.3324 ± 0.0108	1700 ± 50	1620 ± 140			
M1	0.67	1.01 ± 0.06*	0.091 ± 0.004⁺	467 ± 19	460 ± 40	0.23 ± 0.02	0.28 ± 0.03	Non-competitive
	1.33	1.007 ± 0.118*	0.03 ± 0.002§	160 ± 10	160 ± 30			
M2	0.67	1.01 ± 0.03*	0.099 ± 0.002⁺	510 ± 10	500 ± 20	0.25 ± 0.04	0.28 ± 0.02	Non-competitive
	1.33	1.02 ± 0.05*	0.0587 ± 0.0016§	303 ± 8	300 ± 20			
M3	0.1	0.71 ± 0.05	0.119 ± 0.005	610 ± 20	860 ± 80	0.09 ± 0.03	0.133 ± 0.009	Mixed type
	0.33	0.73 ± 0.03	0.073 ± 0.002⁺	377 ± 14	520 ± 40			
L3	0.1	1.08 ± 0.05*	0.032 ± 0.002§¥	164 ± 5	150 ± 10			

	0.67	0.97	±	0.17*	0.02	±	0.002	100	±	10	100	±	30	0.014 ± 0.001	0.0106 ± 0.0008	Non-competitive
L2	0.005	1.08	±	0.14*	0.29	±	0.04	1490	±	190	1380	±	50	0.010 ± 0.002	0.015 ± 0.003[e]	Non-competitive
	0.01	1.011	±	0.014*	0.162	±	0.005	840	±	30	830	±	20			
	0.04	1.2	±	0.2*	0.038	±	0.008¥	200	±	40	167	±	4			

[a] Michaelis-Menten constant, dependent of enzyme concentration. [b] Reaction rate, dependent on enzyme concentration. [c] Catalytic constant, $k_{cat}=v_{max}/[E]$. [d] Catalytic efficiency, calculated by k_{cat}/K_M. [e] For L2, K_i cannot be determined directly from the usual Dixon plot, "K_i" is a more complex function which varies with [I] (K_i^{slope}). *+§¥ There are no statistically significant differences for $p < 0.05$.

It is noticeable that the compounds M1 and M2, both similar in their structure, perform a similar inhibition over PPO with no statistical differences between them. The Michaelis Menten constant maintain the values of the control yet the v_{max} drops off as the amount of inhibitor increases in the solution. This behaviour indicates that both ligand M1 and M2 acts as non-competitive inhibitors. Besides, it seems that the presence of the pyridine in the structure of M2 does not offer additional inhibitory capability to the ligand.

In comparison with M1 and M2, M3 offers an extra inhibition power and also a change in the interaction on the PPO. It seems that the increase in the ring size and the extra nitrogen in its structure improve the inhibitory activity of the PPO. In this case, it was necessary to decrease the concentration to 0.33 mM to obtain the same v_{max} as M1 and M2 with a double concentration (0.66 mM). Furthermore, K_m also drops off with a significant difference from the control meaning that the inhibition would be mixed type in contrast to M1 and M2.

Next ligand with more inhibition power was L3, which has a 24-membered macrocycle ring, ten nitrogens in total and two naphtha-2-ylmethyl units in its structure. With a concentration of 0.1 mM the maximum rate of the tyrosinase decreases approximately

350 to 0.03 mM min^{-1}, also decreasing in a substantial way the catalytic constant and the
351 catalytic efficiency. Thus, L3 is four times more active than M3 and thirteen times more
352 active than M2 and M1. It supports that when increasing the macrocycle size and the
353 number of nitrogens in the macrocycle, together with the presence of the naphth-2-
354 ylmethyl units, the inhibition power rises as deduced from the PLS analysis.
355 Lastly, L2 has also two naphth-2-ylmethyl units but in contrast with L3, they are directly
356 attached to the ring removing two NH units. This ligand is the most powerful inhibitor
357 of the ten tested ligands. The values of K_M and v_{max} were calculated for three different
358 concentrations of L2 (see table 2 and figure 5a). In all the cases a value of K_M around 1.0
359 mM of substrate was obtained, with no statistically significant differences for $p<0.05$ in
360 any case. However, the value of v_{max} decreases from 0.29 to 0.038 mM min^{-1} when
361 increasing the concentration of L2 in the medium. K_M does not vary with the
362 concentration of inhibitor but v_{max} decreases. Thus, we can conclude that L2 induces a
363 non-competitive inhibition over the PPO enzyme where there is no coordination with
364 the active centre. The catalytic efficiency (k_{cat}/K_M) and the turnover number (k_{cat}) follow
365 the same trend as the v_{max}, with values close to 1400 mM min^{-1} in absence of the
366 inhibitor that dropped off up to 150 mM min^{-1} indicating that the efficiency of the
367 enzyme is much lower in the presence of L2 at 0.04 mM, the lowest concentration of all
368 the compounds. Furthermore, the IC_{50} parameter was also estimated at 10 ± 2 µM (n=3)
369 statistically equal to kojic acid in the same conditions.
370 This result indicates that, in general, the interaction of the compounds with the enzyme
371 is not carried out in the active centre, only M3 presents a mixed type inhibition. This
372 absence of direct interaction could be explained since copper is found in the active site
373 of the enzyme, within a biological structure with a complex quaternary structure and

not as a free ion. Although the interaction of the inhibitor with the enzyme is not carried out in the active centre, it is likely to modify the interaction of the substrate with the active centre, avoiding or delaying the formation of products of the reaction [40]

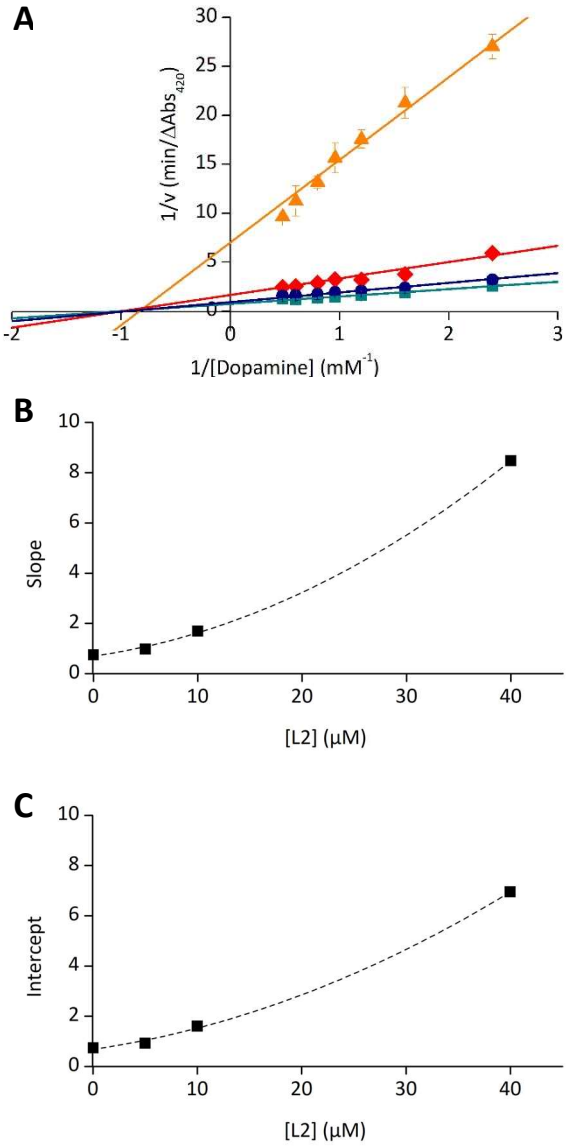

Figure 5: A) Lineaweaver-Burk plot of dopamine oxidation in presence and absence of L2. The concentrations of L2 are (■) 0 μM, (●) 5 μM (◆) 10 μM and (▲) 40 μM. B) Secondary replot of Slope (K_m/V_{max}) vs. [L2]. C) Secondary replot of intercept ($1/V_{max}$) vs [L2]). Data of B) and C) are obtained from A).

3.4. Analysis of L2-mushroom tyrosinase interaction

The influence of the inhibitor in the enzymatic activity was analysed through the study of the variation of the slope and the intercept values with the concentration of L2. In case of conventional Michaelis-Menten systems a linear relationship is found. As can be seen in the figures 5b and 5c, both the slope (K_M/V_{max}) and the intercept ($1/V_{max}$) vs [L2] show an excellent fitting to parabolic (R^2 in both cases is 0.999) instead of linear functions. This indicates that the mechanism is rather an S-parabolic I-parabolic inhibition[41] where there is either a complex non-competitive inhibition with multiple inhibitor sites for one enzyme or complex conformational changes[42,43]. In these cases, K_i cannot be determined directly from the usual plots like Dixon, however, a "K_i" as a more complex function which varies with [I][44,45] ,was determined from equation (2) where K_i is K_i^{slope}.

$$\text{Slope} = K_M/V_{max}\,(1+[I]/K_i)^2 \qquad (2)$$

Applying the equation (1), the K_i^{slope} calculated is 15 ± 3 μM.

Fluorescence studies were also performed in order to get more insight into the nature of the enzyme-inhibitor interactions. It was observed that the intensity of the fluorescence decreases progressively when increasing the amount of L2, although without any ~~no~~ significant shift in the maximum intensity. The Stern-Volmer equation was applied to calculate the Stern-Volmer quenching constant (K_{sv}) and the k_q (biomolecular quenching rate constant) determining whether the mechanism was static or dynamic[46]. The corresponding value for K_{sv} is 7.8 x 10^4 M^{-1} and 7.8 x 10^{12} $M^{-1}s^{-1}$ for k_q. Assuming that the collision quenching constant of biomolecules is about 2.0 x 10^{10} $M^{-1}s^{-1}$, our k_q is two order of magnitude higher, suggesting that the inhibition process provoked for L2 shows a static nature with

a binding between the enzyme and the inhibitor[47]. In this case, the number of binding sites can be obtained by the equation 3[45,48]:

$$\frac{F_0}{F_0 - F} = \frac{1}{n} + \frac{1}{K}\frac{1}{[L1]} \quad (3)$$

Where F_0 and F are the relative fluorescence intensities of the enzyme with and without the inhibitor respectively, [L2] is the concentration of L2, K is the binding constant and n is the number of binding sites. A good correlation was obtained (R^2=0.999) and a value close to 1 (n = 0.860 ± 0.005) was calculated, which indicates the binding of one molecule of L2 to each tyrosinase is enough to change the conformation of the enzyme lowering its activity. Besides a high binding constant was obtained ((1.869 ± 0.018) x 10^5 M^{-1}) in agreement with the great affinity between the enzyme and the inhibitor.

3.5. Inhibitory assays on apple juices as real matrices

Encouraged by the good results offered by L2 as inhibitor of tyrosinase in model systems, its performance was checked in a real food system as it is the case of a freshly obtained apple juice. For that purpose, apples of the c.v. Golden Delicious variety were liquefied and put in contact with two different concentrations (0.5 mM and 1.5 mM) of L2, afterward, the samples were left stirring for one hour. In general terms, once the apples liquefies, the enzymatic browning process begins quickly. The colour change is perceptible to the human eye within the first 5-10 minutes. As we can see in the figure 6a, in absence of inhibitor the juice suffers a strong oxidation of the polyphenols even in the first 10 minutes, changing from bright yellow to an orange colour that becomes reddish after 30 minutes and reaches almost a full oxidative browning after 1 hour.

When the juice is put in contact with the lowest concentration of L2 (0.5 mM) the enzymatic browning is delayed during the first 10 minutes, however, the reaction is not completely stopped and the colour of the juice reaches a browning intensity similar to that observed in the absence of inhibitor at longer times (60 minutes)).

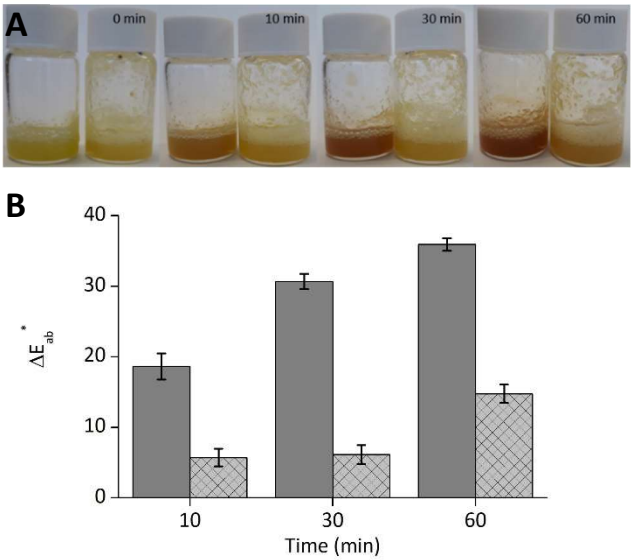

Raising the concentration of L2 in the juice to 1.5 mM, the inhibiting effect of the azamacrocyclic ligand was strong enough to stop the process. The colour change of the juice mixed with the 1.5 mM of L2 is almost inappreciable during the first 30 minutes darkening slightly after 60 minutes.

Figure 6: A) Colour evolution in apple juice without the inhibitor (left) and in the presence of 1.5 mM of L2 (right). B) Measurements of colour difference ΔE over time: control (grey) and with 1.5 mM L2 (striped).

Figure 6b collects the colour change differences (ΔE_{ab}^*) for the apple juice in presence and absence of inhibitor, taking the freshly prepared juice as reference. In agreement with the naked eye colour changes, it can be noticed how after the

446 first 10 minutes the control reaches an ΔEab* close to 20 which continues
447 growing, while the one with inhibitor barely has an ΔEab* of 5 that is maintained
448 during the 30 minutes. At longer times (1 hour) the control shows a colour similar
449 to the 30 minutes indicating that the oxidation is almost complete. However, the
450 sample containing L2 (1.5 mM) holds a significant reduction in the enzymatic
451 browning, although a slight increase in the ΔE_{ab}* is observed suggesting that a
452 residual activity is maintained at long times.
453 In conclusion, during the present study the influence over the enzymatic
454 browning of ten aza-macrocyclic ligands with diverse functionalisation has been
455 tested showing that they can be potentially used as inhibitory products of PPO to
456 a greater or lesser extent. Their chemical structures strongly influence the
457 inhibitory activity being the ring size and the number of nitrogens in the
458 macrocycle (both correlated) the main factor. Also, the presence of bulky
459 aromatic groups attached to the macrocycle was relevant. The inhibition of the
460 enzymatic browning is mainly due to the deactivation of the PPO and suffers a
461 significant rise if the contact time between the enzyme the ligand increases. For
462 L2, the most active inhibitor, kinetic studies indicate that ligands interact with the
463 tyrosinase enzyme with a non-competitive mechanism in a molar proportion of
464 1:1 giving rise to structural change on the protein that provokes an abrupt
465 decrease in its activity. The high inhibitory activity of L2 was verified on a real
466 sample showing how it can reduce the enzymatic browning in an apple juice when
467 used at 1.5 mM. L2 opens the door to a new strategy based on systems that
468 conjugate polyamines and aromatic groups as tyrosinase inhibitors.
469

Acknowledgments

Financial support by the Spanish Ministerio de Ciencia, Innovación y Universidades (project RTI2018-100910-B-C44), Ministerio de Economía y Competitividad (projects CTQ2016-78499-C6-1-R, Unidad de Excelencia MDM 2015-0038 and CTQ2017-90852-REDC) and Generalitat Valenciana (Project PROMETEOII2015-002) is gratefully acknowledged.

References

(1) Simpson, B. K. *Food Biochemistry and Food Processing*; Wiley-Blackwell, 2012.

(2) İyidoğan, N. F.; Bayındırlı, A. Effect of L-Cysteine, Kojic Acid and 4-Hexylresorcinol Combination on Inhibition of Enzymatic Browning in Amasya Apple Juice. *J. Food Eng.* **2004**, *62* (3), 299–304.

(3) Croguennec, T. Enzymatic Browning. In *Handbook of Food Science and Technology 1*; John Wiley & Sons, Inc.: Hoboken, NJ, USA, 2016; pp 159–181.

(4) Brütsch, L.; Rugiero, S.; Serrano, S. S.; Städeli, C.; Windhab, E. J.; Fischer, P.; Kuster, S. Targeted Inhibition of Enzymatic Browning in Wheat Pastry Dough. *J. Agric. Food Chem.* **2018**, *66* (46), 12353–12360.

(5) Ma, L.; Zhang, M.; Bhandari, B.; Gao, Z. Recent Developments in Novel Shelf Life Extension Technologies of Fresh-Cut Fruits and Vegetables. *Trends Food Sci. Technol.* **2017**, *64*, 23–38.

(6) Queiroz, C.; Mendes Lopes, M. L.; Fialho, E.; Valente-Mesquita, V. L. Polyphenol Oxidase: Characteristics and Mechanisms of Browning Control. *Food Rev. Int.* **2008**, *24* (4), 361–375.

(7) Marshall, M.; Kim, J.; Wei, C. Enzymatic Browning in Fruits, Vegetables and

494 Seafoods. *Food Agric. Organ.* **2000**, *41*, 259–312.
495 (8) Seo, S.-Y.; Sharma, V. K.; Sharma, N. Mushroom Tyrosinase: Recent Prospects. *J.*
496 *Agric. Food Chem.* **2003**, *51* (10), 2837–2853.
497 (9) Tronc, J.-S.; Lamarche, F.; Makhlouf, J. Enzymatic Browning Inhibition in Cloudy
498 Apple Juice by Electrodialysis. *J. Food Sci.* **1997**, *62* (1), 75–78.
499 (10) Jiang, S.; Penner, M. H. The Nature of β-Cyclodextrin Inhibition of Potato
500 Polyphenol Oxidase-Catalyzed Reactions. *Food Chem.* **2019**, *298*, 125004.
501 (11) Buckow, R.; Kastell, A.; Terefe, N. S.; Versteeg, C. Pressure and Temperature
502 Effects on Degradation Kinetics and Storage Stability of Total Anthocyanins in
503 Blueberry Juice. *J. Agric. Food Chem.* **2010**, *58* (18), 10076–10084.
504 (12) Massini, L.; Rico, D.; Martin-Diana, A. B. Quality Attributes of Apple Juice: Role
505 and Effect of Phenolic Compounds. In *Fruit Juices*; Rajauria, G., Tiwari, B. K., Eds.;
506 Academic Press, 2018; pp 45–57.
507 (13) McEvily, A. J.; Iyengar, R.; Otwell, W. S. Inhibition of Enzymatic Browning in
508 Foods and Beverages. *Crit. Rev. Food Sci. Nutr.* **1992**, *32* (3), 253–273.
509 (14) Iyengar, R.; McEvily, A. J. Anti-Browning Agents: Alternatives to the Use of
510 Sulfites in Foods. *Trends Food Sci. Technol.* **1992**, *3*, 60–64.
511 (15) Muñoz-Pina, S.; Ros-Lis, J. V.; Argüelles, Á.; Coll, C.; Martínez-Máñez, R.; Andrés,
512 A. Full Inhibition of Enzymatic Browning in the Presence of Thiol-Functionalised
513 Silica Nanomaterial. *Food Chem.* **2018**, *241*, 199–205.
514 (16) Muñoz-Pina, S.; Ros-Lis, J. V.; Argüelles, Á.; Martínez-Máñez, R.; Andrés, A.
515 Influence of the Functionalisation of Mesoporous Silica Material UVM-7 on
516 Polyphenol Oxidase Enzyme Capture and Enzymatic Browning. *Food Chem.*
517 **2020**, *310*, 125741.

(17) Fraschetti, C.; Filippi, A.; Crestoni, M. E.; Marcantoni, E.; Glucini, M.; Guarcini, L.; Montagna, M.; Guidoni, L.; Speranza, M. Protonated Hexaazamacrocycles as Selective K Receptors. *J. Am. Soc. Mass Spectrom.* **2015**, *26* (7), 1186–1190.

(18) Yu, X.; Zhang, J. *Macrocyclic Polyamines : Synthesis and Applications*; WILEY-VCH Verlag, 2017.

(19) Castillo, C. E.; Máñez, M. A.; Basallote, M. G.; Clares, M. P.; Blasco, S.; García-España, E. Copper (II) Complexes of Quinoline Polyazamacrocyclic Scorpiand-Type Ligands: X-Ray, Equilibrium and Kinetic Studies. *Dalt. Trans.* **2012**, *41* (18), 5617.

(20) Santra, S.; Mukherjee, S.; Bej, S.; Saha, S.; Ghosh, P. Amino-Ether Macrocycle That Forms Cu ^{II} Templated Threaded Heteroleptic Complexes: A Detailed Selectivity, Structural and Theoretical Investigations. *Dalt. Trans.* **2015**, *44* (34), 15198–15211.

(21) Malthus, S. J.; Wilson, R. K.; Vikas Aggarwal, A.; Cameron, S. A.; Larsen, D. S.; Brooker, S. Carbazole-Based N 4 -Donor Schiff Base Macrocycles: Obtained Metal Free and as Cu (II) and Ni (II) Complexes. *Dalt. Trans.* **2017**, *46* (10), 3141–3149.

(22) Fan, R.; Serrano-Plana, J.; Oloo, W. N.; Draksharapu, A.; Delgado-Pinar, E.; Company, A.; Martin-Diaconescu, V.; Borrell, M.; Lloret-Fillol, J.; García-España, E.; et al. Spectroscopic and DFT Characterization of a Highly Reactive Nonheme FeV-Oxo Intermediate. *J. Am. Chem. Soc.* **2018**, *140* (11), 3916–3928.

(23) Lincoln, K. M.; Gonzalez, P.; Richardson, T. E.; Julovich, D. A.; Saunders, R.; Simpkins, J. W.; Green, K. N. A Potent Antioxidant Small Molecule Aimed at Targeting Metal-Based Oxidative Stress in Neurodegenerative Disorders. *Chem.*

Commun. **2013**, *49* (26), 2712–2714.

(24) Martínez-Camarena, Á.; Liberato, A.; Delgado-Pinar, E.; Algarra, A. G.; Pitarch-Jarque, J.; Llinares, J. M.; Mañez, M. Á.; Domenech-Carbó, A.; Basallote, M. G.; García-España, E. Coordination Chemistry of Cu $^{2+}$ Complexes of Small N-Alkylated Tetra-Azacyclophanes with SOD Activity. *Inorg. Chem.* **2018**, *57* (17), 10961–10973.

(25) Algarra, A. G.; Basallote, M. G.; Belda, R.; Blasco, S.; Castillo, C. E.; Llinares, J. M.; García-España, E.; Gil, L.; Máñez, M. Á.; Soriano, C.; et al. Synthesis, Protonation and Cu ^{II} Complexes of Two Novel Isomeric Pentaazacyclophane Ligands: Potentiometric, DFT, Kinetic and AMP Recognition Studies. *Eur. J. Inorg. Chem.* **2009**, *2009* (1), 62–75.

(26) Díaz, P.; Basallote, M. G.; Máñez, M. A.; García-España, E.; Gil, L.; Latorre, J.; Soriano, C.; Verdejo, B.; Luis, S. V. Thermodynamic and Kinetic Studies on the Cu (II) Coordination Chemistry of a Novel Binucleating Pyridinophane Ligand. *Dalt. Trans.* **2003**, No. 6, 1186–1193.

(27) Basallote, M. G.; Doménech, A.; Ferrer, A.; García-España, E.; Llinares, J. M.; Máñez, M. A.; Soriano, C.; Verdejo, B. Synthesis and Cu(II) Coordination of Two New Hexaamines Containing Alternated Propylenic and Ethylenic Chains: Kinetic Studies on PH-Driven Metal Ion Slippage Movements. *Inorganica Chim. Acta* **2006**, *359* (7), 2004–2014.

(28) Acosta-Rueda, L.; Delgado-Pinar, E.; Pitarch-Jarque, J.; Rodríguez, A.; Blasco, S.; González, J.; Basallote, M. G.; García-España, E. Correlation between the Molecular Structure and the Kinetics of Decomposition of Azamacrocyclic Copper(II) Complexes. *Dalt. Trans.* **2015**, *44* (17), 8255–8266.

(29) Alarcón, J.; Albelda, M. T.; Belda, R.; Clares, M. P.; Delgado-Pinar, E.; Frías, J. C.; García-España, E.; González, J.; Soriano, C. Synthesis and Coordination Properties of an Azamacrocyclic Zn(II) Chemosensor Containing Pendent Methylnaphthyl Groups. *Dalt. Trans.* **2008**, No. 46, 6530–6538.

(30) Clares, M. P.; Aguilar, J.; Aucejo, R.; Lodeiro, C.; Albelda, M. T.; Pina, F.; Lima, J. C.; Parola, A. J.; Pina, J.; Seixas de Melo, J.; et al. Synthesis and H^{+}, Cu^{2+}, and Zn^{2+} Coordination Behavior of a Bis(Fluorophoric) Bibrachial Lariat Aza-Crown. *Inorg. Chem.* **2004**, *43* (19), 6114–6122.

(31) Siddiq, M.; Dolan, K. D. Characterization and Heat Inactivation Kinetics of Polyphenol Oxidase from Blueberry (Vaccinium Corymbosum L.). *Food Chem.* **2017**, *218*, 216–220.

(32) Vermeer, L. M.; Higgins, C. A.; Roman, D. L.; Doorn, J. A. Real-Time Monitoring of Tyrosine Hydroxylase Activity Using a Plate Reader Assay. *Anal. Biochem.* **2013**, *432* (1), 11–15.

(33) Espín, J. C.; Varón, R.; Fenoll, L. G.; Gilabert, M. A.; García-Ruíz, P. A.; Tudela, J.; García-Cánovas, F. Kinetic Characterization of the Substrate Specificity and Mechanism of Mushroom Tyrosinase. *Eur. J. Biochem.* **2000**, *267* (5), 1270–1279.

(34) Doran, P. M. *Principios de Ingeniería de Los Bioprocesos*; Acribia, 1998.

(35) Marcantoni, E.; Petrini, M. Recent Developments in the Stereoselective Synthesis of Nitrogen-Containing Heterocycles Using *N* -Acylimines as Reactive Substrates. *Adv. Synth. Catal.* **2016**, *358* (23), 3657–3682.

(36) Liu, W.; Zou, L.; Liu, J.; Zhang, Z.; Liu, C.; Liang, R. The Effect of Citric Acid on the Activity, Thermodynamics and Conformation of Mushroom Polyphenoloxidase.

590 *Food Chem.* **2013**, *140* (1–2), 289–295.
591 (37) Son, S. M.; Moon, K. D.; Lee, C. Y. Kinetic Study of Oxalic Acid Inhibition on
592 Enzymatic Browning. *J. Agric. Food Chem.* **2000**, *48* (6), 2071–2074.
593 (38) ÖZ, F.; COLAK, A.; ÖZEL, A.; SAĞLAM ERTUNGA, N.; SESLI, E. PURIFICATION AND
594 CHARACTERIZATION OF A MUSHROOM POLYPHENOL OXIDASE AND ITS ACTIVITY
595 IN ORGANIC SOLVENTS. *J. Food Biochem.* **2013**, *37* (1), 36–44.
596 (39) Ayaz, F. A.; Demir, O.; Torun, H.; Kolcuoglu, Y.; Colak, A. Characterization of
597 Polyphenoloxidase (PPO) and Total Phenolic Contents in Medlar (Mespilus
598 Germanica L.) Fruit during Ripening and over Ripening. *Food Chem.* **2008**, *106*
599 (1), 291–298.
600 (40) Harvey, R. A.; Ferrier, D. R. *Biochemistry*; Wolters Kluwer Health/Lippincott
601 Williams & Wilkins, 2011.
602 (41) Fromm, H. J. Chapter 10: Reversible Enzyme Inhibitors as Mechanistic Probes. In
603 *Contemporary enzyme kinetics and mechanism: Reliable Lab Solutions*; Purich, D.
604 L., Ed.; Elsevier/Academic Press: Ney York, 2009; pp 279–302.
605 (42) Segel, I. H. *Enzyme Kinetics : Behavior and Analysis of Rapid Equilibrium and*
606 *Steady State Enzyme Systems*; Wiley Classics Library: New York, 1993.
607 (43) Qin, X.-Y.; Lee, J.; Zheng, L.; Yang, J.-M.; Gong, Y.; Park, Y.-D. Inhibition of α-
608 Glucosidase by 2-Thiobarbituric Acid: Molecular Dynamics Simulation
609 Integrating Parabolic Noncompetitive Inhibition Kinetics. *Process Biochem.* **2018**,
610 *65*, 62–70.
611 (44) Chakrabarty, S. P.; Ramapanicker, R.; Mishra, R.; Chandrasekaran, S.; Balaram, H.
612 Development and Characterization of Lysine Based Tripeptide Analogues as
613 Inhibitors of Sir2 Activity. *Bioorg. Med. Chem.* **2009**, *17* (23), 8060–8072.

(45) Gou, L.; Lee, J.; Yang, J.-M.; Park, Y.-D.; Zhou, H.-M.; Zhan, Y.; Lü, Z.-R. Inhibition of Tyrosinase by Fumaric Acid: Integration of Inhibition Kinetics with Computational Docking Simulations. *Int. J. Biol. Macromol.* **2017**, *105*, 1663–1669.

(46) Tang, H.; Cui, F.; Li, H.; Huang, Q.; Li, Y. Understanding the Inhibitory Mechanism of Tea Polyphenols against Tyrosinase Using Fluorescence Spectroscopy, Cyclic Voltammetry, Oximetry, and Molecular Simulations. *RSC Adv.* **2018**, *8* (15), 8310–8318.

(47) Dewey, T. G. *Biophysical and Biochemical Aspects of Fluorescence Spectroscopy*; Plenum Press, 1991.

(48) Gou, L.; Lee, J.; Hao, H.; Park, Y.-D.; Zhan, Y.; Lü, Z.-R. The Effect of Oxaloacetic Acid on Tyrosinase Activity and Structure: Integration of Inhibition Kinetics with Docking Simulation. *Int. J. Biol. Macromol.* **2017**, *101*, 59–66.